VIP Carbon Nitrides Very Important Paper

Deutsche Ausgabe: DOI: 10.1002/ange.201511217
Internationale Ausgabe: DOI: 10.1002/anie.201511217

Phenyl-Modified Carbon Nitride Quantum Dots with Distinct Photoluminescence Behavior

Qianling Cui, Jingsan Xu, Xiaoyu Wang, Lidong Li,* Markus Antonietti, and Menny Shalom*

Abstract: *A novel type of quantum dot (Ph-CN) is manufactured from graphitic carbon nitride by "lining" the carbon nitride structure with phenyl groups through supramolecular preorganization. This approach requires no chemical etching or hydrothermal treatments like other competing nanoparticle syntheses and is easy and safe to use. The Ph-CN nanoparticles exhibit bright, tunable fluorescence, with a high quantum yield of 48.4 % in aqueous colloidal suspensions. Interestingly, the observed Stokes shift of approximately 200 nm is higher than the maximum values reported for carbon nitride based fluorophores. The high quantum yield and the large Stokes shift are related to the structural surface organization of the phenyl groups, which affects the π-electron delocalization in the conjugated carbon nitride networks and induces colloidal stability. The remarkable performance of the Ph-CN nanoparticles in imaging is demonstrated by a simple incubation study with HeLa cells.*

In the last years, metal-free graphene-based materials with high biocompatibility, apparently low toxicity, and unique optical properties have been considered to be promising candidates to replace traditional metal-containing quantum dots in bioimaging and biomedical applications.[1] However, the large-scale chemical preparation of graphene-based nanomaterials is far from being simple and usually involves the use of corrosive and toxic agents, while the resulting materials exhibit relatively low photoresponse. Furthermore, the origins (quantum confinement, surface states, size effects) of the optical properties are still under debate.[2] Therefore, it is still rewarding to search for new metal-free materials with high fluorescence efficiency.

A metal-free analogue is graphitic carbon nitride with an ideal stoichiometry of C_3N_4, which is set up from layered (tri-*s*-)triazine units. Graphitic carbon nitride (referred to as CN) has attracted enormous attention as a polymeric semiconductor in photocatalysis and electrocatalysis in the last decade.[3] Nevertheless, most of these applications focus on the use of macroscopic materials with micrometer-sized particles, and the usage of nanosized CN quantum dots in bioimaging and biomedicine, for example, has been limited by their low photoluminescence (PL) quantum efficiency.[4] In the last years, several methods were successfully introduced to enhance the fluorescence efficiency. However, these methods rely on the use of concentrated acid/base processes, etching, and/or hydro/solvothermal cutting, and in some cases, the emission even fell back into the ultraviolet region.[5] Therefore, a facile, mild, and more environmentally friendly preparation method for highly fluorescent CN is still required. Ideally, this method should enable us to tune the PL properties (such as the Stokes shift) of the CN nanoparticles and achieve emission in the visible range. Large Stokes shifts can improve the fluorescence efficiency owing to the drop in reabsorption events that lead to non-radiative recombination. Thus far, the maximum reported Stokes shift for CN is 130 nm, whereas values of 100 nm are commonly observed, and there is significant overlap between the absorption and emission spectra.[4a]

Recently, we have developed a supramolecular preorganization approach to template the structure and improve the photocatalytic activities of CN.[6] The electronic and optical properties of the final CN materials can be optimized by the careful design and selection of the supramolecular starting complex; for example, the use of a cyanuric acid/melamine assembly also enables the integration of other molecules, such as barbituric acid,[7] urea,[8] and even caffeine.[9] We also showed the power of this method by using a complex with phenyl-substituted triazines to grow modified CN thin films as the active layers in solar cells and light-emitting diodes,[10] applications that rely on the control of the band structure and the emission properties.

Herein, we use this synthetic approach for the preparation of CN quantum dots with high fluorescence efficiency and large Stokes shifts. The phenyl groups that were incorporated into the CN framework play a key role in tailoring the optical behavior. Aqueous suspensions of the CN nanoparticles were prepared by the simple approach that is illustrated in the Supporting Information, Figure S1. First, bulk samples were synthesized according to our previous report by heating a complex of cyanuric acid and 2,4-diamino-6-phenyl-1,3,5-triazine (barbituric acid can also be added) in nitrogen atmosphere.[10b] After cooling, the obtained yellow powders were exfoliated by simple ultrasonication in a water bath, followed by centrifugation to remove the residual big aggregates. Colloidal suspensions with high transparency (Figure S1) were obtained; the phenyl-decorated CN materials without and with barbituric acid are referred to as Ph-CN

[*] Dr. Q. Cui, Dr. X. Wang, Prof. Dr. L. Li
State Key Laboratory for Advanced Metals and Materials
School of Materials Science and Engineering
University of Science and Technology Beijing
Beijing 100083 (China)
E-mail: lidong@mater.ustb.edu.cn
Dr. J. Xu, Prof. Dr. M. Antonietti, Dr. M. Shalom
Department of Colloid Chemistry
Max Planck Institute of Colloids and Interfaces
14424 Potsdam (Germany)
E-mail: Jingsan.Xu@mpikg.mpg.de

Supporting information and the ORCID identification number(s) for the author(s) of this article can be found under http://dx.doi.org/10.1002/anie.201511217.

and Ph-CNB, respectively. The addition of barbituric acid introduces more carbon atoms into the CN frameworks and leads to a red shift of the PL spectra.[11]

The morphology of the Ph-CN colloidal nanoparticles was characterized by transmission electron microscopy (TEM, Figure 1 a), which showed nanosheets with lateral dimensions below 100 nm. Atomic force microscopy (AFM) demonstrated that the thickness of these nanosheets goes down to 5–6 nm, indicating that the Ph-CN nanoparticles comprise 15–20 CN layers. The size distribution determined by dynamic light scattering (DLS) reveals a mean hydrodynamic diameter of approximately 70 nm (Figure 1 b), which is in accordance with the TEM and AFM observations. Zeta potential measurements demonstrate that the nanoparticles are highly negatively charged, with a zeta potential of -38.0 ± 0.5 mV. The isoelectric point of the nanoparticles was measured to be 4.5, which agrees well with previously reported values for CN materials.[12] The strong electrostatic repulsion between these nanoparticles endows them with excellent stability in aqueous solution, and a homogeneous dispersion remained stable for more than one year under ambient conditions. The good dispersibility and high stability of the CN colloids are favorable for investigations of their optical properties and applications in bioimaging. Powder X-ray diffraction (XRD) and Fourier transform infrared spectroscopy (FT-IR) were performed to determine the lattice structure and functional groups of Ph-CN before and after exfoliation. As depicted in Figure 1 e, both the bulk material and the nanoparticles display a diffraction peak at 27.4°, which corresponds to an interlayer distance of 0.33 nm between the planar carbon nitride sheets. The decreased diffraction intensity of the nanoparticles reflects the fact that the vertical stacking of CN layers is restricted by the exfoliation process.[13,14] We prolonged the sonication time further to 24 hours and found only a slight intensity decrease for the diffraction peak (Figure S2), indicating that the sonication treatment could not completely destroy the crystal structure of CN. The strong vibration bands at 1200–1600 cm^{-1} and 802 cm^{-1} in the FT-IR spectra (Figure 1 f) are attributed to the stretching modes of the CN heterocycles and the vibration of the heptazine units, respectively.[15] Importantly, solid-state ^{13}C NMR spectra clearly show that at least significant parts of the phenyl groups from the precursor were successfully incorporated into the CN networks, as additional chemical shifts were observed at 129 and 133 ppm aside from the ones for ordinary CN (Figure S3).[16]

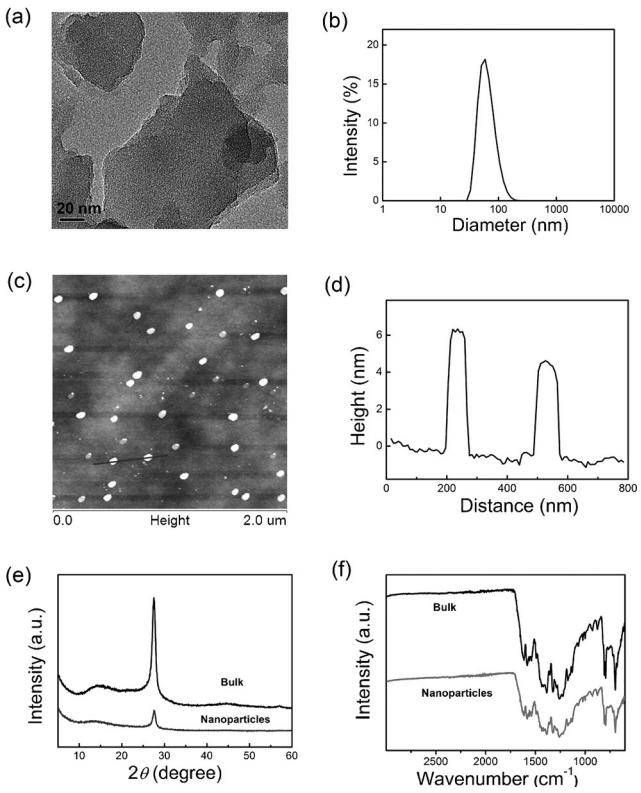

Figure 1. a) TEM image, b) size distribution determined by DLS, and c) AFM image of the synthetized Ph-CN nanoparticles. d) The corresponding height profile of two random nanoparticles from the AFM image. e) XRD pattern and f) FTIR spectra of Ph-CN bulk material and Ph-CN nanoparticles.

The optical properties of the CN aqueous suspensions were studied by UV/Vis absorption and PL spectroscopy. The UV/Vis spectra of the Ph-CN nanoparticles feature a sharp absorption edge at 400 nm and reach their maximum absorbance at around 300 nm (Figure 2 a), showing a significant blue shift compared to the bulk counterpart (Figure S4). This shift is usually attributed to size effects, which cause the conduction band (CB) and the valence band (VB) to move in

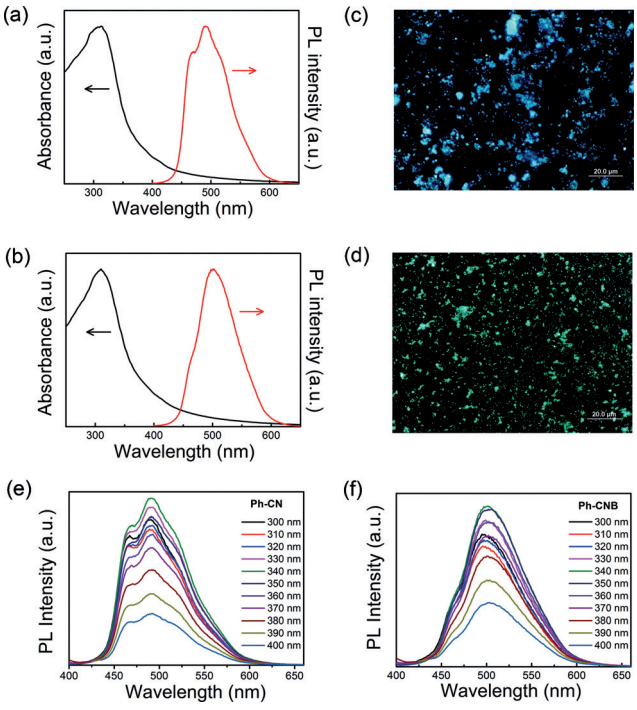

Figure 2. a, b) UV/Vis and PL spectra of colloidal dispersions of Ph-CN (a) and Ph-CNB (b). c, d) Luminescence microscopy images of Ph-CN (c) and Ph-CNB (d) nanoparticles dispersed on a glass substrate obtained with an optical microscope under UV illumination. e, f) PL spectra of colloidal Ph-CN (e) and Ph-CNB (f) upon excitation at wavelengths from 300 to 400 nm.

opposite directions.[4a] Upon excitation at 340 nm, the Ph-CN nanosheets generate a PL spectrum in the range of 450 to 600 nm, with a main emission peak at 490 nm and a small shoulder at 470 nm (Figure 2a). The Ph-CNB suspension shows an absorption spectrum that is similar to that of Ph-CN. Its PL spectrum shows a further red shift of approximately 15 nm with respect to Ph-CN while the shoulder at 470 nm is diminished (Figure 2b). We surmise that the weakening of the shoulder peak should be related to surface defect states, which are likely to arise from the replacement of N by C in the Ph-CN framework, which in turn is induced by the addition of barbituric acid during the synthesis of CN. The defect sites result in the quenching of the transition that corresponds to the shoulder peak as well as in the red shift of the main peak.[3c] As a result, dispersions of Ph-CN and Ph-CNB nanoparticles display strong cyan and green emission, respectively (Figure 2c,d) under UV irradiation. The PL spectra obtained upon excitation at $\lambda = 300$–400 nm indicate no peak shifts, while the strongest emission was achieved under 340 nm excitation for both Ph-CN and Ph-CNB (Figure 2e,f).

The absolute emission quantum yield (QY) of the Ph-CN colloidal nanoparticles was determined to be as high as 48.4% using an integrating sphere, a rather pleasing value compared to those previously reported for other CN luminescent materials.[17] It should be emphasized that in comparison to previous methods, no hydrothermal treatment or hazardous chemicals were necessary in the presented approach, which renders it safe, robust, and highly suitable for large-scale preparations. The Ph-CNB quantum dots still demonstrate a relativity high QY of 30.9% despite the introduction of defect sites (the optimal emission QY of the bulk species was below 20%).[10a] Further evidence for the superior emission properties was obtained by time-resolved PL analysis of the Ph-CN and Ph-CNB colloidal suspensions, which determined their average fluorescence lifetimes to be 51 and 21 ns, respectively. These values indicate that the excitons are highly stable and do not find non-radiative emission channels within the nanoparticles even on these longer time scales. It is important to note that these values are higher than those of many known dyes and comparable to those of traditional, metal-based core–shell fluorescent quantum dots.[18] Another important feature of the CN quantum dots is the large Stokes shift of up to 200 nm, which is much higher than usually observed (ca. 100 nm) for carbon nitride and other carbon materials.[17] Both a long fluorescence lifetime and a large Stokes shift are also suited to comply with the requirements of advanced optical super-resolution techniques, such as stimulated emission depletion (STED).[19]

The high fluorescence QY of the Ph-CN nanoparticles can be attributed to several factors: 1) The quantum confinement effect in the quantum dots. As illustrated by Xie et al.,[4a] nanosized CN has a much enhanced PL efficiency compared to the bulk counterpart, simply because the number of defects per particle is low. 2) The effects of the phenyl groups. The phenyl groups attached to the CN framework enable extended π-electron delocalization in the conjugated structure, which improves the PL efficiency.[20] In earlier work, we had utilized bulk Ph-CN as the active layer in light-emitting diodes, and interestingly, the phenyl groups induced a strong red shift (170 nm) of the electroluminescence compared to the PL owing to the formation of additional surface levels.[10a] However, because of the large bulk to surface ratio of this material, the PL was dominated by bulk effects, and the surface structure did not play a crucial role. On the contrary, in the present colloidal system, the ratio of the surface to bulk states is dramatically increased because of the small size of the CN particles. These surface states, presumably related to a rather tight capping with the phenyl groups, offer optical transitions that are within the classical bulk band gap of pure carbon nitride. This hypothesis was further confirmed by the large Stokes shift, which clearly indicates that the emission does not result from the CB–VB transition, but from a lower-energy state, which then of course also does not depend on bulk defects, as they are energetically not accessible anymore. Such a transition mode involving surface structures has also been described for the emission of organic molecules[21] as well as quantum dots.[22] Furthermore, we believe that the large Stokes shift partially results from the strong interactions between the excitons and the distorted crystal lattice (as noted above) of the CN nanoparticles, resulting in energy loss by heat dissipation before the excitons recombine radiatively.[23] Therefore, the emitted photons are lower in energy than the absorbed photons, and an unusually large Stokes shift is observed.

To further confirm our assumptions, we measured the absorption and emission spectra of CN colloids that were made from non-phenyl-containing precursors, including dicyandiamide, melamine, and cyanuric acid/melamine supramolecular complexes. We found that all of these CN nanoparticles showed a much lower QY (below 10%) along with significantly decreased Stokes shifts (ca. 130 nm; see Figure S5). These results confirm that the phenyl groups and their potential enrichment at the particle surface indeed contribute to improving the fluorescence of the CN materials.

The exfoliation process was also carried out in some other solvents to study the effects of the liquid medium on the PL of the Ph-CN nanoparticles. As the solvent polarity was decreased, the stability of the CN suspensions was reduced significantly. In non-polar solvents such as hexane and toluene, the nanoparticles quickly aggregated and precipitated. In solvents with medium polarity, such as tetrahydrofuran (THF), ethanol, and dimethylformamide (DMF), the colloidal suspensions remained stable for a few days. Among the tested solvents, only water could disperse the CN nanoparticles for longer periods of time (more than 12 months), which was ascribed to the Coulomb stabilization of the nanoparticles in water.[4a] It is important to note that in THF, the Ph-CN suspension was more stable than normal CN, further confirming the presence of phenyl groups on the material surface (Figure S6). The normalized PL spectra of the suspensions in water, DMF, ethanol, and THF (Figure S7) show that the solvent has only a slight impact on the emission peaks of the CN nanoparticles, suggesting that the emission does not originate from solvation effects but is most likely solely due to the nanoparticle structure. In water, the PL intensity depends on the pH value and decreases steeply when the pH is above 7, in the absence of any peak shift (Figure S8). The reduced emission at higher pH can be

attributed to 1) the acidic properties of the fluorescent species in CN, 2) the formation of defects, and 3) interactions of electrons or holes with the solvent. It is well known that carbon nitrides can create oxy radicals under illumination in water, for example, for the photodegradation of dyes.[6a] This process partly relies on the transfer of electrons from the CB of CN to dissolved dioxygen, which leads to the formation of a superoxide radical. Furthermore, the enlarged band gap of the Ph-CN quantum dots indicates the movement of the band positions in opposite directions, which hence thermodynamically enables the reaction between the holes and hydroxy groups to form hydroxyl radicals. In this scenario, O_2 and OH^- can act as electron/hole scavengers, and thus the PL is significantly quenched at high pH values.

The cytotoxicity of an imaging agent is an important parameter to evaluate its practical application. Here, the cytotoxicity of as-prepared CN nanoparticles towards HeLa cells was tested by a standard MTT assay after incubation with different amounts of the colloids for 24 hours. As shown in Figure 3a, more than 80% of the cells remained alive in the presence of Ph-CN over the tested concentration range, whereas Ph-CNB showed slightly decreased toxicity compared to Ph-CN. Considering their low cytotoxicity and enhanced PL properties, these as-obtained CN nanoparticles might be a promising emitting agent for in vitro bioimaging.

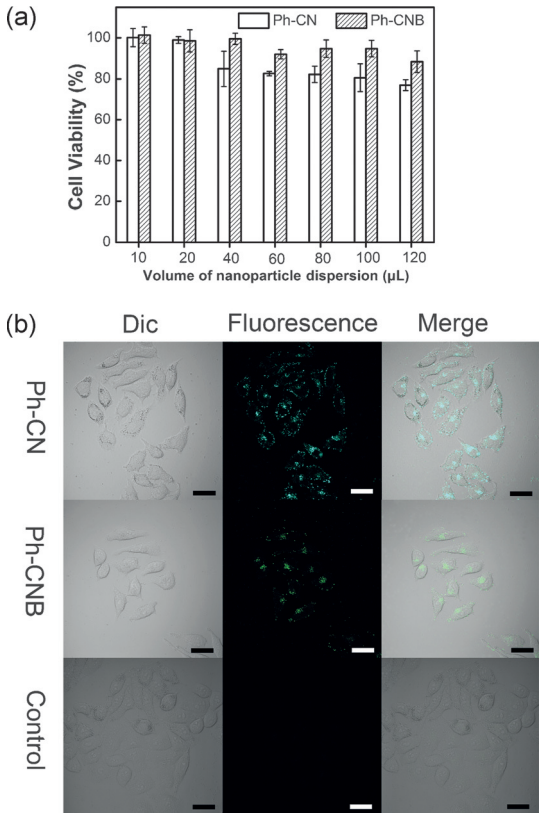

Figure 3. a) Cell viability after incubation of HeLa cells with various volumes of CN colloidal dispersions. b) Optical field, confocal fluorescence, and merged images of HeLa cells incubated with Ph-CN or Ph-CNB or with no nanoparticle treatment in DMEM medium for 10 h. The images were obtained using a 405 nm laser, and the fluorescence signals were collected from 450 nm to 550 nm. Scale bars: 20 μm.

Then, bioimaging experiments were carried out with HeLa cells after incubation with the as-obtained CN nanoparticles at 37 °C for 10 hours. The confocal fluorescence image in Figure 3b shows that HeLa cells incubated with Ph-CN exhibit bright cyan emission upon excitation at 405 nm. The optical images indicated the good condition of the HeLa cells without observable damage from these CN nanoparticles. Furthermore, the merged image revealed that the Ph-CN nanoparticles were well taken up by HeLa cells. Similar phenomena were also observed for the Ph-CNB nanoparticles, but with green fluorescence. Taking their small size and good biocompatibility into account, these unfunctionalized CN nanoparticles are most likely transported into cells by endocytosis.[24]

In summary, the simple synthesis of CN quantum dots with a high fluorescence quantum yield (up to 48%), a long fluorescence lifetime of 51 ns, and an unusually large Stokes shift of 200 nm has been achieved by the use of phenyl-containing supramolecular precursors. The significantly enhanced photoresponse compared to previous reports is assumed to originate from the introduction of phenyl groups, especially at the particle surface, which induces surface capping and lower electronic energy states that direct the photoluminescence and avoid non-radiative recombination. Because of their intense fluorescence, low cytotoxicity, and excellent dispersity, the CN colloids were employed as imaging agents with cyan/green fluorescence for bioimaging. We believe that this work can open the door for the replacement of metal-based fluorescent nanomaterials (i.e., quantum dots) in many biomedicine-related applications because of the simple and effective synthetic approach as well as the low cost of carbon nitride materials.

Acknowledgements

Q.C. and L.L. are grateful to the National Natural Science Foundation of China (51503015).

Keywords: carbon nitrides · cell imaging · colloidal suspensions · fluorescence · Stokes shifts

How to cite: *Angew. Chem. Int. Ed.* **2016**, *55*, 3672–3676
Angew. Chem. **2016**, *128*, 3736–3740

[1] J. Shen, Y. Zhu, X. Yang, C. Li, *Chem. Commun.* **2012**, *48*, 3686–3699.

[2] a) S. Zhu, J. Zhang, C. Qiao, S. Tang, Y. Li, W. Yuan, B. Li, L. Tian, F. Liu, R. Hu, *Chem. Commun.* **2011**, *47*, 6858–6860; b) V. Strauss, J. T. Margraf, C. Dolle, B. Butz, T. J. Nacken, J. Walter, W. Bauer, W. Peukert, E. Spiecker, T. Clark, D. M. Guldi, *J. Am. Chem. Soc.* **2014**, *136*, 17308–17316.

[3] a) Y. Zheng, L. Lin, B. Wang, X. Wang, *Angew. Chem. Int. Ed.* **2015**, *54*, 12868–12884; *Angew. Chem.* **2015**, *127*, 13060–13077; b) Y. Zheng, Y. Jiao, S. Z. Qiao, *Adv. Mater.* **2015**, *27*, 5372–5378; c) J. Zhang, X. Chen, K. Takanabe, K. Maeda, K. Domen, J. D. Epping, X. Fu, M. Antonietti, X. Wang, *Angew. Chem. Int. Ed.* **2010**, *49*, 441–444; *Angew. Chem.* **2010**, *122*, 451–454; d) J. Zhang, M. Zhang, L. Lin, X. Wang, *Angew. Chem. Int. Ed.* **2015**, *54*, 6297–6301; *Angew. Chem.* **2015**, *127*, 6395–6399; e) J.

Zhang, Y. Chen, X. Wang, *Energy Environ. Sci.* **2015**, *8*, 3092 – 3108.
[4] a) X. Zhang, X. Xie, H. Wang, J. Zhang, B. Pan, Y. Xie, *J. Am. Chem. Soc.* **2013**, *135*, 18 – 21; b) X. Zhang, H. Wang, H. Wang, Q. Zhang, J. Xie, Y. Tian, J. Wang, Y. Xie, *Adv. Mater.* **2014**, *26*, 4438 – 4443; c) S. Yang, Y. Gong, J. Zhang, L. Zhan, L. Ma, Z. Fang, R. Vajtai, X. Wang, P. M. Ajayan, *Adv. Mater.* **2013**, *25*, 2452 – 2456.
[5] a) J. Zhou, Y. Yang, C.-Y. Zhang, *Chem. Commun.* **2013**, *49*, 8605 – 8607; b) Z. Zhou, Y. Shen, Y. Li, A. Liu, S. Liu, Y. Zhang, *ACS Nano* **2015**, *9*, 12480 – 12487; c) W. Wang, C. Y. Jimmy, Z. Shen, D. K. Chan, T. Gu, *Chem. Commun.* **2014**, *50*, 10148 – 10150; d) Z. Song, T. Lin, L. Lin, S. Lin, F. Fu, X. Wang, L. Guo, *Angew. Chem. Int. Ed.* **2016**, DOI: 10.1002/anie.201510945; *Angew. Chem.* **2016**, DOI: 10.1002/ange.201510945.
[6] a) M. Shalom, S. Inal, C. Fettkenhauer, D. Neher, M. Antonietti, *J. Am. Chem. Soc.* **2013**, *135*, 7118 – 7121; b) Y. Ishida, L. Chabanne, M. Antonietti, M. Shalom, *Langmuir* **2014**, *30*, 447 – 451.
[7] M. Shalom, M. Guttentag, C. Fettkenhauer, S. Inal, D. Neher, A. Llobet, M. Antonietti, *Chem. Mater.* **2014**, *26*, 5812 – 5818.
[8] Y. Liao, S. Zhu, J. Ma, Z. Sun, C. Yin, C. Zhu, X. Lou, D. Zhang, *ChemCatChem* **2014**, *6*, 3419 – 3425.
[9] T. Jordan, N. Fechler, J. Xu, T. J. K. Brenner, M. Antonietti, M. Shalom, *ChemCatChem* **2015**, *7*, 2826 – 2830.
[10] a) J. Xu, M. Shalom, F. Piersimoni, M. Antonietti, D. Neher, T. J. K. Brenner, *Adv. Opt. Mater.* **2015**, *3*, 913 – 917; b) J. Xu, T. J. K. Brenner, L. Chabanne, D. Neher, M. Antonietti, M. Shalom, *J. Am. Chem. Soc.* **2014**, *136*, 13486 – 13489.
[11] J. Qin, S. Wang, H. Ren, Y. Hou, X. Wang, *Appl. Catal. B* **2015**, *179*, 1 – 8.
[12] B. Zhu, P. Xia, W. Ho, J. Yu, *Appl. Surf. Sci.* **2015**, *344*, 188 – 195.
[13] a) A. Thomas, A. Fischer, F. Goettmann, M. Antonietti, J.-O. Müller, R. Schlögl, J. M. Carlsson, *J. Mater. Chem.* **2008**, *18*, 4893 – 4908; b) S. Barman, M. Sadhukhan, *J. Mater. Chem.* **2012**, *22*, 21832 – 21837; c) X. Wang, K. Maeda, A. Thomas, K. Takanabe, G. Xin, J. M. Carlsson, K. Domen, M. Antonietti, *Nat. Mater.* **2009**, *8*, 76 – 80.
[14] a) L. Lin, Z. Cong, J. Li, K. Ke, S. Guo, H. Yang, G. Chen, *J. Mater. Chem. B* **2014**, *2*, 1031 – 1037; b) H. Zhang, Y. Huang, S. Hu, Q. Huang, C. Wei, W. Zhang, L. Kang, Z. Huang, A. Hao, *J. Mater. Chem. C* **2015**, *3*, 2093 – 2100.
[15] J. R. Holst, E. G. Gillan, *J. Am. Chem. Soc.* **2008**, *130*, 7373 – 7379.
[16] J. Zhang, M. Zhang, S. Lin, X. Fu, X. Wang, *J. Catal.* **2014**, *310*, 24 – 30.
[17] a) Y.-P. Sun, B. Zhou, Y. Lin, W. Wang, K. A. S. Fernando, P. Pathak, M. J. Meziani, B. A. Harruff, X. Wang, H. Wang, P. G. Luo, H. Yang, M. E. Kose, B. Chen, L. M. Veca, S.-Y. Xie, *J. Am. Chem. Soc.* **2006**, *128*, 7756 – 7757; b) L. Tang, R. Ji, X. Cao, J. Lin, H. Jiang, X. Li, K. S. Teng, C. M. Luk, S. Zeng, J. Hao, S. P. Lau, *ACS Nano* **2012**, *6*, 5102 – 5110.
[18] U. Resch-Genger, M. Grabolle, S. Cavaliere-Jaricot, R. Nitschke, T. Nann, *Nat. Methods* **2008**, *5*, 763 – 775.
[19] J. Hanne, H. J. Falk, F. Gorlitz, P. Hoyer, J. Engelhardt, S. J. Sahl, S. W. Hell, *Nat. Commun.* **2015**, *6*, 7127 – 7132.
[20] B. Valeur, *Molecular Fluorescence: Principles and Applications*, Wiley-VCH, Weinheim, **2001**.
[21] a) D. M. Shcherbakova, M. A. Hink, L. Joosen, T. W. J. Gadella, V. V. Verkhusha, *J. Am. Chem. Soc.* **2012**, *134*, 7913 – 7923; b) W. Bi, X. Li, L. Zhang, T. Jin, L. Zhang, Q. Zhang, Y. Luo, C. Wu, Y. Xie, *Nat. Commun.* **2015**, *6*, 8647 – 8653.
[22] L. Li, A. Pandey, D. J. Werder, B. P. Khanal, J. M. Pietryga, V. I. Klimov, *J. Am. Chem. Soc.* **2011**, *133*, 1176 – 1179.
[23] a) B. Henderson, G. F. Imbusch, *Optical Spectroscopy of Inorganic Solids*, Oxford University Press, Oxford, **1989**; b) N. B. Hannay, *Treatise on Solid State Chemistry*, *Vol. 2 Defects in Solids*, Plenum Press, New York, **1975**.
[24] S. Zhang, H. Gao, G. Bao, *ACS Nano* **2015**, *9*, 8655 – 8671.

Received: December 3, 2015
Revised: January 23, 2016
Published online: February 15, 2016

